Earthquakes and Structures, *Vol. 14, No. 4 (2018) 313-322*
DOI: https://doi.org/10.12989/eas.2018.14.4.313

Response of anisotropic porous layered media with uncertain soil parameters to shear body-and Love-waves

Amina Sadouki[*1], Zamila Harichane[1a], Sidi Mohammed Elachachi[2a] and Ayfer Erken[3a]

[1]*Geomaterials Laboratory, Hassiba Benbouali University of Chlef, Algeria*
[2]*University of Bordeaux, I2M, GCE Department, France*
[3]*Civil Engineering Faculty, Istanbul Technical University, Turkey*

(Received September 25, 2017, Revised February 22, 2018, Accepted February 23, 2018)

Abstract. The present study is dedicated to investigate the *SH* body-as well as *Love*-waves propagation effects in porous media with uncertain porosity and permeability. A unified formulation of the governing equations for one-dimensional (1-D) wave propagation in anisotropic porous layered media is presented deterministically. The uncertainties around the above two cited parameters are taken into account by random fields with the help of Monte Carlo Simulations (MCS). Random samples of the porosity and the permeability are generated according to the normal and lognormal distribution functions, respectively, with a mean value and a coefficient of variation for each one of the two parameters. After performing several thousands of samples, the mathematical expectation (mean) of the solution of the wave propagation equations in terms of amplification functions for *SH* waves and in terms of dispersion equation for *Love*-waves are obtained. The limits of the *Love* wave velocity in a porous soil layer overlaying a homogeneous half-space are obtained where it is found that random variations of porosity change the zeros of the wave equation. Also, the increase of uncertainties in the porosity (high coefficient of variation) decreases the mean amplification function amplitudes and shifts the fundamental frequencies. However, no effects are observed on both *Love* wave dispersion and amplification function for random variations of permeability. Lastly, the present approach is applied to a case study in the Adapazari town basin so that to estimate ground motion accelerations lacked in the fast-growing during the main shock of the damaging 1999 Kocaeli earthquake.

Keywords: *SH* wave; *Love* wave; dispersion; Monte Carlo simulations; amplification; acceleration

1. Introduction

Various important issues such as site amplification, dispersion and attenuation of seismic waves are related directly or indirectly to seismic waves propagation. In recent years, the wave propagation in porous media has received great interest in soil dynamics and acoustics (Rohan 2013). In particular, problems related to shear-waves propagation in porous media are of great practical interest. Rao Rama and Sarma (1984) discussed the problem of generation of *SH* waves due to a shear stress discontinuity at the interface of a layered half-space of poroelastic materials. Sharma and Gogna (1993) considered the reflection and refraction of *SH* waves in an initially stressed medium consisting of a sandy layer laying over a fluid-saturated porous solid half-space. Pallavika *et al*. (2008) used the finite difference method to model the propagation of *SH*-waves in a multilayered porous media for different values of anisotropy and porosity parameters of the medium. Ghorai *et al.* (2010) studied the propagation of *Love* waves in a fluid saturated porous layer under a rigid boundary and laying over an elastic half-space under gravity, and mainly discussed the lower and upper bounds of *Love* waves velocity. Bansal and Kuldeepak (2011) derived the dispersion equation which relates the phase velocity to the wave number, the shear wave velocities of the layers, the anisotropy factors, and the non-homogeneity characteristic of the lower semi-infinite half-space, based on the propagation of *SH*-type waves in a multilayer fluid-saturated porous stratum. Son and Kang (2012) investigated the propagation of shear waves in a transversely isotropic poroelastic layer constrained between two elastic layers and Gupta *et al.* (2013) studied the propagation of *Love* wave in an initially stressed orthotropic medium sandwiched by a homogeneous and a non-homogeneous semi-infinite media. In both works, the dispersion equation for shear waves has been derived and it was shown the dependency of the phase velocities on the medium characteristics such as porosity and anisotropy. Kakar (2015) studied the *SH*-wave propagation in a heterogeneous layer laying over an inhomogeneous isotropic elastic half-space and observed that the velocity of *SH*-wave increases with the increase of the inhomogeneity parameter.

On other hand, natural (or inherent) variability of soil properties and the heterogeneities in pore fluid can produce significant attenuation and dispersion in the low-frequency seismic range (Ren *et al.* 2009). So, soil properties such as density, shear moduli and damping coefficients are prone to uncertainties and a deterministic analysis may not be suitable (Assimaki *et al.* 2003) since the uncertainties in the properties of the medium induce uncertainties in the

∗Corresponding author, Assistant Professor
E-mail: amina_sadouki@yahoo.fr
[a]Professor

ISSN: 2092-7614 (Print), 2092-7622 (Online)

predicted responses. Consequently, site amplification study will not be complete if the influence of random spatial variations of soil properties and in some cases the soil saturation level are not included in the analysis. In fact, Guellil *et al.* (2017) showed that random variations of thickness and shear wave velocity of a soil layer over bedrock significantly affect the impedance functions and the soil-foundation-structure response.

Sidhu (1971) studied the propagation of *Love* waves in a two-layered heterogeneous half-space and draw the dispersion curves taking into account the variation of elastic parameters with depth to conclude that the minimum group velocity due to heterogeneity occurs at a value of the period smaller than for the homogeneous model. Wang and Hao (2002) investigated the effects of random variations of soil properties on site amplification of seismic waves due to *SH* wave or combined *P* and *SV* waves considering shear modulus, damping ratio, mass density, as well as ground water level as random variables. They showed that the estimated surface motions differ substantially with random variations of soil properties. Saha *et al.* (2015) derived the frequency equation and showed that the heterogeneity and the porosity of the porous half-space have notable effect on the propagation of *Love* waves.

This paper focuses a unified formulation of the propagation of body *SH* or surface *Love* waves in a transversely anisotropic fluid-saturated porous medium in the (x, z) plane, due to usefulness of *SH*- waves and *Love*-waves in practice. The porous medium parameters (porosity and permeability) are assumed uncertain and modeled as random variables not because the medium is random but because these uncertainties are usually modeled by random fields described by their probability density functions (PDFs) or their statistical moments (i.e., mean value and coefficient of variation (C_v) (Bezih *et al*. 2015). In fact, the formulation and solution of the equations of motion due to the propagation of these wave types are often performed separately in the literature, whereas they can be treated in a similar way and only attention should be paid to the boundary conditions.

The formulation is carried into a deterministic context and the effects of uncertainties around the porosity and the permeability are taken into consideration using Monte Carlo Simulations (MCSs). Firstly, the dispersion equation of *Love*-waves is investigated. Then, the soil amplification due to the propagation of *SH*-body waves are studied and discussed. Lastly, this approach is applied to estimate ground motions at Adapazari town city in Turkey due to the unavailability of strong ground motions records during the main shock of the 17 August, 1999 Kocaeli earthquake which severely damaged this area where soft soil-deposits were assumed to have large effects on such damage.

2. Basic equations

For a fluid-saturated anisotropic dissipative porous medium without body forces, the equations of motion are (Biot 1956a, b).

$$\sigma_{ij,j} = \rho_{11}\ddot{u}_i + \rho_{12}\ddot{U} - b_{ij}\left(\dot{U}_j - \dot{u}_j\right) \tag{1a}$$

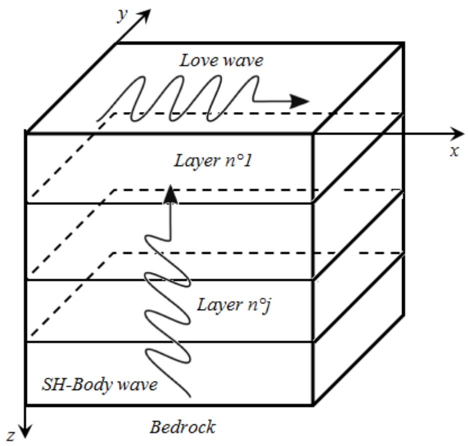

Fig. 1 One dimensional geometrical soil model and wave pattern

$$\sigma_{ij,j} = \rho_{11}\ddot{u}_i + \rho_{12}\ddot{U}_i - b_{ij}\left(\dot{U}_j - \dot{u}_j\right) \tag{1b}$$

Where σ_{ij} are the components of the stress tensor in the solid skeleton (solid phase), $\sigma=\phi p$ is the reduced pressure of the fluid. p is the pressure in the fluid, and ϕ the porosity of the porous medium. $u_i, U_i, \dot{u}_i, \dot{U}_i, \ddot{u}_i, \ddot{U}_i$, ($i, j=x, y, z$) are the solid skeleton and the pore fluid displacement, velocity, and acceleration components, respectively, according to Cartesian coordinates (Fig. 1), and b_{ij} are the dissipation coefficients. The mass coefficients ρ_{11}, ρ_{12} and ρ_{22} take into account the inertia effects of the moving fluid and are associated with the densities of the solid (ρ_S) and the fluid (ρ_f) by the following mixtures relationships

$$\rho_{11} = (1-\phi)\,\rho_s - \rho_{12} \tag{2a}$$

$$\rho_{22} = \phi\,\rho_f - \rho_{12} \tag{2b}$$

$$\rho_{12} = \phi\,(1-a)\rho_f \tag{2c}$$

Where $a = \frac{1}{2}(1+\frac{1}{\phi})$ is the dynamic tortuosity so that the bulk density is given by

$$\rho = \phi\,\rho_f + (1-\phi)\rho_s \tag{2d}$$

The dynamic coefficients obey to the inequalities

$$\rho_{11} > 0, \quad \rho_{12} \le 0, \quad \rho_{22} > 0, \quad \rho_{11}\rho_{22} - \rho_{12}^2 > 0 \tag{2e}$$

The constitutive equations for the transversely anisotropic fluid-saturated porous medium with orthotropic symmetry (Ghorai *et al.* 2010) may be expressed in terms of displacement vectors of solid skeleton and pore fluid as

$$\sigma_{xx} = 2N\,\varepsilon_{xx} + A\,e + Q\,E \tag{3a}$$

$$\sigma_{yy} = 2N\,\varepsilon_{yy} + A\,e + Q\,E \tag{3b}$$

$$\sigma_{zz} = 2N\,\varepsilon_{zz} + A\,e + Q\,E \tag{3c}$$

$$\sigma_{xy} = 2N\,\varepsilon_{xy} \tag{3d}$$

$$\sigma_{yz} = 2G\,\varepsilon_{yz} \tag{3e}$$

$$\sigma_{xz} = 2G\,\varepsilon_{xz} \tag{3f}$$

$$\sigma = -\phi\, p = Q e + RE \tag{3g}$$

Where the components of the strain tensor are

$$\varepsilon_{ij} = \frac{1}{2}\left(\frac{\partial u_i}{\partial x_j} + \frac{\partial u_j}{\partial x_i}\right) \tag{4a}$$

while e and E are the corresponding dilatations

$$e = \varepsilon_{xx} + \varepsilon_{yy} + \varepsilon_{zz} \tag{4b}$$

$$E = \frac{\partial U_x}{\partial x} + \frac{\partial U_y}{\partial y} + \frac{\partial U_z}{\partial z} \tag{4c}$$

A, G, N are the elastic coefficients of the solid skeleton, R is the elastic coefficient of the fluid, and Q is the coupling elastic coefficient between the fluid phase and the solid phase.

So, the resulting out-of plane displacements in the following forms may considerably simplify the boundary value problem (Ghorai *et al.* 2010, Son *et al.* 2012)

$$u_x = u_z = 0\,, u_y = u\,(x,z,t) \tag{5a}$$

$$U_x = U_z = 0\,, U_y = U(x,z,t) \tag{5b}$$

Under these assumptions, the constitutive equations become

$$\sigma_{xx} = \sigma_{yy} = \sigma_{zz} = \sigma_{xz} = 0 \tag{6a}$$

$$\sigma_{xy} = 2N\frac{\partial u}{\partial x} \tag{6b}$$

$$\sigma_{yz} = 2G\frac{\partial u}{\partial z} \tag{6c}$$

With the help of Eq. (6) and setting $b_{22}=b$ ($b = \phi^2 \dfrac{\upsilon}{\kappa}$ where κ is Darcy's permeability coefficient and υ the absolute viscosity), Eqs. (1a) and (1b) become

$$N\frac{\partial^2 u}{\partial x^2} + G\frac{\partial^2 u}{\partial z^2} = \rho_{11}\ddot{u}_2 + \rho_{12}\ddot{U}_2 - b\,\left(\dot{U}_2 - \dot{u}_2\right) \tag{7a}$$

$$\rho_{12}\ddot{u}_2 + \rho_{22}\ddot{U}_2 + b\left(\dot{U}_2 - \dot{u}_2\right) = 0 \tag{7b}$$

For harmonic *shear* wave, propagating in the (x, z) plane, the displacements can take the form

$$\begin{Bmatrix} u(x,z,t) \\ U(x,z,t) \end{Bmatrix} = \begin{Bmatrix} u_0\,(z) \\ U_0\,(z) \end{Bmatrix} e^{i(k_x l_x x + k_z l_z z - wt)} \tag{8}$$

such that $u_0(z)$ and $U_0(z)$ are the displacement amplitudes in the solid and the fluid. i is the complex number ($i^2=-1$), l_x and l_z are the direction cosines, ω is the circular frequency, and k_l ($l=x$, z) the wave number in the x- and z- directions, respectively.

3. Deterministic solutions

3.1 Solution for body vertical SH wave

For body *SH* wave propagating vertically ($l_x=0$, $l_z=I$), Eq. (8) becomes

$$\begin{Bmatrix} u(x,z,t) \\ U(x,z,t) \end{Bmatrix} = \begin{Bmatrix} v_0(z) \\ V_0(z) \end{Bmatrix} e^{-i\omega t} \tag{9}$$

with

$$\begin{Bmatrix} v_0(z) \\ V_0(z) \end{Bmatrix} = \begin{Bmatrix} u_0(z)\, e^{i k_z z} \\ U_0(z)\, e^{i k_z z} \end{Bmatrix} \tag{10}$$

Incorporating Eq. (9) in Eqs. (7-a) and (7-b) leads to the following wave equation:

$$\left(\frac{d^2}{dz^2} + k_z^{\,2}\right) v_0(z) = 0 \tag{11}$$

In Eq. (11), k_z is the wave number ($k_z = \dfrac{\omega}{V_\beta}$), and V_β is the *SH* body shear wave velocity of the fluid-saturated porous medium in the z direction obtained as

$$V_\beta = \sqrt{\frac{G\left(\rho_{22} - \dfrac{ib}{\omega}\right)}{\left(\rho_{11}\rho_{22} - \rho_{12}^2\right) - \dfrac{ib}{\omega}\left(\rho_{11} + \rho_{22} + 2\rho_{12}\right)}} \tag{12}$$

All the above equations are established for a soil layer overlaying a half-space. For a multilayer medium consisting of several horizontal layers, all the equations hold by adding an index j (number of the concerned layer, j=1, N where N is the number of layers laying on a half-space or bedrock). The solution of Eq. (11) is well known under the form

$$v_0(z_j) = A_j e^{i k_{zj} z_j} + A'_j e^{-ik_{zj} z_j} \tag{13}$$

Where A_j and A_j' are the incident and reflected wave amplitude, respectively, in each layer j which can be obtained from the boundary conditions.

3.2 Solution for horizontal Love wave

For horizontal *Love* wave ($l_x=1$, $l_z=0$) propagating in an anisotropic soil layer over bedrock, Eq. (8) becomes

$$\begin{Bmatrix} u(x,z,t) \\ U(x,z,t) \end{Bmatrix} = \begin{Bmatrix} u_0(z) \\ U_0(z) \end{Bmatrix} e^{i(k_x - \omega t)} \tag{14}$$

Using Eq. (14), Eqs. (7a) and (7b) take the form

$$\left(\frac{d^2}{dx^2} + k_x^{\,2}\right) u_0(z) = 0 \tag{15}$$

Where k_x is the wave number in the x direction.

$$k_x^{\,2} = \left(\frac{\alpha}{Gk^2} - \frac{N}{G} \right) k^2 \tag{16a}$$

or

$$k_x^{\,2} = \frac{N}{G} \left(\frac{\alpha}{Nk^2} - 1 \right) k^2 \tag{16b}$$

and $k = \dfrac{\omega}{V_\alpha}$ with V_α the velocity of the *Love* wave. The parameter α is obtained as

$$\alpha = \frac{\left(\rho_{11}\rho_{22} - \rho_{12}^2\right) - \dfrac{ib}{\omega}\left(\rho_{11} + \rho_{22} + 2\rho_{12}\right)}{\rho_{22} - \dfrac{ib}{\omega}} \tag{17}$$

In the case of non-viscous layer (b=0), $\alpha=\omega^2.d'$ with $d' = \rho_{11}\rho_{22} - \rho_{12}^2$ and k_x^2 takes the following form as also obtained by (Ghorai *et al.* 2010)

$$k_x^{\,2} = \frac{N}{G} \left(\frac{V^2}{V_\alpha^{'2}} - 1 \right) k^2 \tag{18a}$$

In Eq. (18a), V_α' is the shear wave velocity in the x direction ($V_\alpha' = \sqrt{N/d'}$). Alternatively, k_x^2 may be written as

$$k_x^{\,2} = \gamma d \left(\frac{V^2}{V_{\alpha_1}^{\,2}} - \frac{1}{d} \right) k^2 \tag{18b}$$

so that $V_{\alpha_1} = \sqrt{N/\rho'}$, $V_\alpha' = V_{\alpha_1}\sqrt{1/d}$, and $\gamma=N/G$. $V_{\alpha 1}$ is the shear wave velocity in the corresponding non porous anisotropic elastic medium in the x direction.

If the medium is composed of N horizontal anisotropic layers, the solution of Eq. (15) is obtained in the form

$$u_0(z_j) = C_j e^{i k_{x_j} z_j} + C_j' e^{-i k_{x_j} z_j} \tag{19}$$

Where C_j and C_j' are the incident and reflected wave amplitudes, respectively, in each layer j which may be obtained from boundary conditions (Crampin 1970, Kielczynski *et al.* 2015).

3.3 Boundary conditions

Generated shear displacements and stresses by *SH*-body waves and *Love* waves propagating in an anisotropic multilayer must satisfy the following boundary conditions:

(1) Nullity of shear stress at free surface ($\sigma_{yz}(z_1=0)=0$), leading to the equality of incident and reflected wave amplitudes in the surface layer: $A_1' = A_1$ and $C_1' = C_1$.

(2) Satisfaction of continuity of shear displacements ($v_{0j}(z_j = h_j) = v_{0j+1}(z_{j+1} = 0)$, $u_{0j}(z_j = h_j) = u_{0j+1}(z_{j+1} = 0)$) and stresses ($\sigma_{yz_j}(z_j = h_j) = \sigma_{yz_{j+1}}(z_{j+1} = 0)$) at each interface between two successive layers leading to

$$A_{j+1} = \frac{1}{2} A_j \left(1 + q_j\right) e^{ik_{z_j} h_j} + \frac{1}{2} A_j' \left(1 - q_j\right) e^{-k_{z_j} h_j} \tag{20a}$$

$$A_{j+1}' = \frac{1}{2} A_j \left(1 - q_j\right) e^{ik_{z_j} h_j} + \frac{1}{2} A_j' \left(1 + q_j\right) e^{-k_{z_j} h_j}$$

$$\begin{aligned} C_{j+1} &= \frac{1}{2} C_j \left(1 + q_j\right) e^{ik_{x_j} h_j} + \frac{1}{2} C'_j \left(1 - q_j\right) e^{-k_{x_j} h_j} \\ C_{j+1} &= \frac{1}{2} C_j \left(1 - r_j\right) e^{ik_{z_j} h_j} + \frac{1}{2} C_j' \left(1 + r_j\right) e^{-k_{x_j} h_j} \end{aligned} \tag{20b}$$

with $q_j = \sqrt{\rho_j G_j / \rho_{j+1} G_{j+1}}$

(3) For *Love* waves, at large distances ($z\to\infty$) from the free surface (z=0) the generated displacement should tend to zero, i.e., $u_0(z\to\infty)=0$ (Kielczynski 2018) so that $C_{N+1}=0$, and the displacement in the half-space is then

$$u_0(z_{N+1}) = C_{N+1}' e^{-ik_{x_{N+1}} z_{N+1}} \tag{21}$$

3.4 Dispersion equation

For *Love* wave, the boundary conditions for a soil layer over a bedrock, are rewritten in the following form

$$\begin{cases} C_1 - C_1' = 0 \\ C_1 e^{ik_{x1}h_1} + C_1' e^{ik_{x1}h_1} - C_2' = 0 \\ C_1 e^{ik_{x1}h_1} - C_1' e^{-ik_{x1}h_1} + \dfrac{G_2 k_{x_2}}{G_1 k_{x_1}} C_2' = 0 \end{cases} \tag{22}$$

This system has a non-zero solution only if the determinant is null which gives

$$tg\left[\sqrt{\gamma d . \left(\frac{V^2}{V_{\alpha_1}^{\,2}} - \frac{1}{d} \right)} k h_1 \right] = i \frac{G_2}{G_1} \left[\sqrt{\frac{\dfrac{N_2}{G_2}\left(\dfrac{V^2}{V_{\alpha_2}^{\,2}} - 1 \right)}{\gamma d \left(\dfrac{V^2}{V_{\alpha_1}^{\,2}} - \dfrac{1}{d} \right)}} \right] \tag{23a}$$

or

$$tg\left[\sqrt{\gamma d . \left(1 - \frac{1}{d} \frac{V_{\alpha_1}^{\,2}}{V^2} \right)} \frac{\omega h_1}{V_{\alpha_1}} \right] = i \frac{G_2}{G_1} \left[\sqrt{\frac{\dfrac{N_2}{G_2}\left(\dfrac{V^2}{V_{\alpha_2}^{\,2}} - 1 \right)}{\gamma d \left(\dfrac{V^2}{V_{\alpha_1}^{\,2}} - \dfrac{1}{d} \right)}} \right] \tag{23b}$$

Eqs. (23a) or (23b) are called dispersion equation of *Love* wave in a porous anisotropic layered media. For a layered isotropic nonporous media ($N_2=G_2$, $V_{\alpha 1}=V_{S1}$, $V_{\alpha 2}=V_{S2}$, d=1, γ=1) Eq. (23b) becomes

$$tg\left[\sqrt{1 - \frac{V_{S_1}^{\,2}}{V^2}} \frac{\omega h_1}{V_{S_1}} \right] = i \frac{G_2}{G_1} \sqrt{\frac{\dfrac{V^2}{V_{S_2}^{\,2}} - 1}{\dfrac{V^2}{V_{S_1}^{\,2}} - 1}} \tag{23c}$$

In Eq. (23-c), $V_{S_1} = \sqrt{G_1/\rho_1}$ and $V_{S_2} = \sqrt{G_2/\rho_2}$ are the velocities of the shear wave in the non-porous isotropic: (1) layer material and (2) half-space, respectively.

Begin

Initialize data (read mean and standard deviation values of each parameter)

For i = 1 to m **do** (*m is the number of frequencies*)

$f(i)=(i-1)^*\,\Delta f$

For nr = 1 to Nrun **do** (*Nrun is the number of trials in Monte Carlo procedure*)

- Generate Nrun normally distributed parameters for porosity (ϕ) or lognormally distributed for the permeability (K)
- Calculate the amplification function for *SH*-body wave
- or solve the dispersion equation for *L*ove wave

end for

- Calculate mean response for *SH*-body wave (amplification function, acceleration, …)
- or obtain shear wave velocity limits for *L*ove wave

end for

end

Fig. 2 Algorithm of the Monte Carlo simulations of the dynamic response of a anisotropic porous layered media

4. Monte Carlo simulations for uncertain selected parameters

In order to take into account the uncertainties due to the inherent variability of soil properties, it is suggested to model some parameters associated with the porous medium structure (porosity and permeability) as random variables according to predefined distribution function. So, the governing equations are solved several thousands time with the aid of Monte Carlo Simulations (MCSs). Each one of the two selected parameters is treated as a random variable.

After performing several thousands of samples of one or more random parameters, the mathematical expectations of the velocity, amplification function, or transient response of the considered system is obtained as elucidated in Fig. 2.

5. Results and discussions

5.1 Love waves velocity limits in a porous media with uncertain parameters

In this section, it is expected to study the equation of dispersion of *Love* waves in a porous anisotropic soil layer with random porosity and permeability. Table 1 shows the input frequency independent parameters for a porous layer of 30 m thickness laying over an elastic half-space. In table 1, C_v refers to the coefficient of variation of a parameter. The case of C_v=0% represents the deterministic case, i.e., no fluctuations around the parameter are considered.

This study concerns the determination of the lower and upper bounds of the *Love* wave velocity given their great importance in both theoretical and practical aspects (Ghorai *et al.* 2010). *Love* waves may be considered as a powerful tool for materials evaluation such as in non-destructive testing (NDT) and geophysics practical applications

Table 1 Parameters for a porous layer

	Porosity ϕ		Permeability K (m/s)		Mass density (kg/m^3)		viscosity υ (kg/m.s)	Shear moduli (Pa)
	mean	C_v (%)	mean	C_v (%)	ρ_S	ρ_f		
Hard soil	0.30	0 10 20 30	10^{-3}	0 20 40 60 80	2000	1000	0,001	5.10^8
Soft soil	0.55		10^{-7}					5.10^7

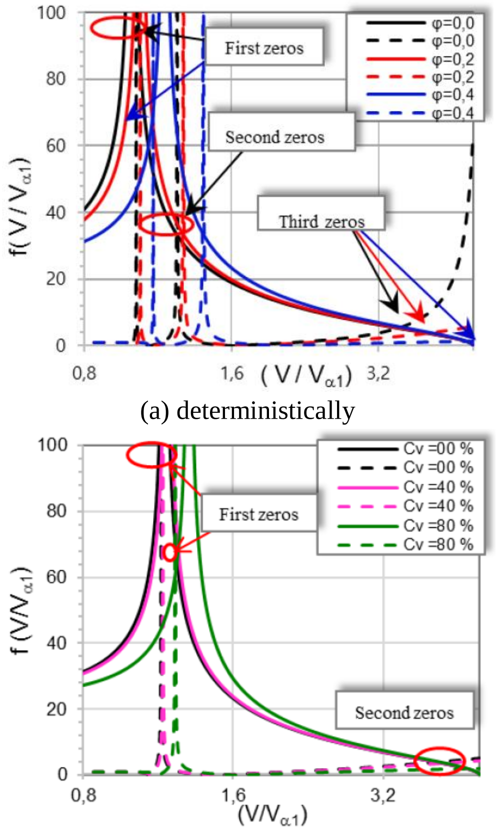

Fig. 3 Determination of the limits of the *Love* wave velocity for a porous layer over an elastic half-space for porosity variation: The solid line refers to left side of Eq. (23c) and dashed line refers to right side of Eq. (23c)

(Kielczynski *et al.* 2015). The role of the porosity of the medium in the existence or non-existence of *Love* waves is indicated by the parameter *d*.

In fact, the layer is porous when $0<d<1$, non-porous solid when $d\rightarrow1$, and tends to be fluid when $d\rightarrow0$. The unknown values of the wave velocity $V/V_{\alpha1}$ have been obtained by determining the intersection points of the two functions in the left and right hand side of the dispersion Eq. (23b), as shown in Fig. 3(a).

Firstly, the dispersion equation is solved deterministically for non-viscous soil layer (b=0) overlaying an isotropic elastic half-space. Two parameters govern the dispersion equation: $V/V_{\alpha1}$ and V/V_{S2}. The

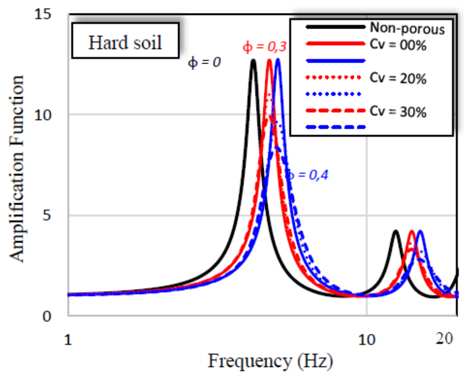

(a) Hard soil

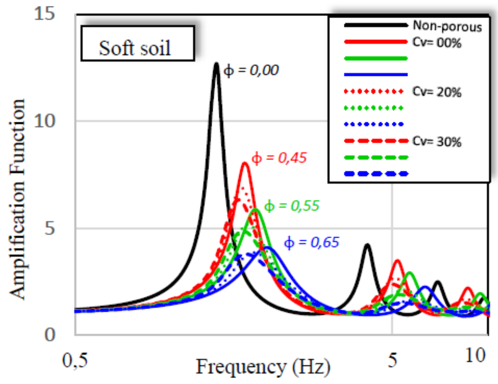

(b) Soft soil

Fig. 4 Effects of porosity variations on amplification function of hard and soft soil layers

dispersion equation is plotted in Fig. 3(a) for a ratio V_{S1}/V_{S2}=5, $\omega h/V_{S1}$=8, and three values of the porosity: 0 value (elastic non porous layer), 0.2 value (relatively elastic porous layer), and 0.4 value (elastic porous layer). The mass density of the layer is close to that of the half-space ($\rho_1=\rho_2$). Several solutions of the wave equation may be obtained depending on V_{S1}/V_{S2} and $\omega h/V_{S1}$. The locations of the intersection points on the figure show that for this intermediate case of vibration ($\omega h/V_{S1}$=8), the first zeros are close to V_{S1} as porosity decrease which means that the *Love* wave velocity is dominated by that of the layer. But the others zeros are close to that of the half-space as the porosity increases. So, for highly porous media the wave velocity is dominated by that of the half-space.

Secondly, the dispersion equation is solved for the parameters varying randomly. Mean curves of the two functions are traced versus $V/V_{\alpha 1}$ for several C_v of porosity in Fig. 3(b). It is observed that moderate fluctuations about porosity (up to 40%) do not exert significant effect on the velocity of the *Love* wave. While for the high random variation (C_v=80%), the wave velocity approaches to that of the half space. So, the random variations of porosity change the zeros of the wave equation.

5.2 Effect of parameters' uncertainties on the amplification function of SH-waves

In this section, it is intended to investigate the effects of the uncertainty of the porous media properties (porosity and

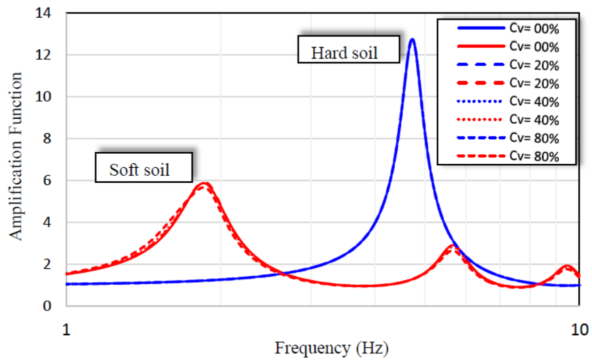

Fig. 5 Effects of permeability variations on amplification function of hard and soft soil layers

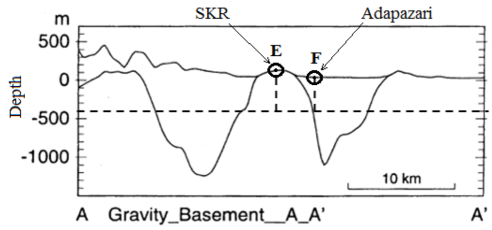

Fig. 6 Cross-section for gravity-basement and surface topography (Komazawa *et al.* 2002)

permeability) on the amplification of seismic waves in the same previous environments (Table 1) but for two kinds of materials: hard soil and soft soil. The uncertain parameters are also modeled as random variables.

Figs. 4 and 5 depict the effects of random variations of porosity and permeability, respectively, on the mean amplification function magnitudes. It may be concluded that random variations of permeability do not exert significant effects on mean amplification functions. However, for different values of mean porosity, the mean amplification function amplitudes decrease as the C_v of porosity increases for hard soil. But for the soft soil, for different mean values of porosity, the mean amplification function amplitudes decrease as the C_v of porosity increases and the fundamental frequencies are shifted towards left.

6. A case study in Adapazari city, 1999 Kocaeli earthquake

6.1 Brief overview on Adapazari city and 1999 Kocaeli earthquake

During the 17 August 1999 Kocaeli earthquake, an event of magnitude M=7.4, buildings in the urban/industrial area of the Adapazari basin were severely damaged (Celebi *et al.* 2000). This earthquake caused extensive liquefaction-induced ground deformations along the coasts of Sapanca Lake (Cetin *et al.* 2002). Adapazari has been developed on young flood-plain-deposits of Sakarya River. Therefore, soft soil-deposits were thought to have large effects on such damage (Komazawa *et al.* 2000). The cross section of gravity-basement and surface topography around the Adapazari site is shown in Fig. 6.

Table 2 Input data of the SKR and Adapazari soil profiles

SKR rock Site (E)				
Layer number	Thickness layer (m)	Wave velocity (m/s)	Mass density (kg/m3)	Damping (%)
1	72	1050	2500	7
2	56	1500	2500	7
Base rock	-	2000	2500	7
Adapazari soft site (F)				
Layer number	Thickness layer (m)	Wave Velocity (m/s)	Mass density (kg/m3)	Damping (%)
1	65	200	1700	7
2	90	500	1800	7
3	250	1000	2000	7
Base rock	-	3500	2500	7

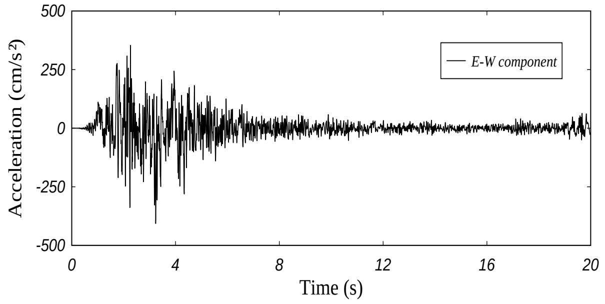

Fig. 7 Recorded accelerations at the Sakarya station (SKR-site E) during the August 17, 1999 Kocaeli mainshock earthquake

The strong motion sites, Sakarya (SKR) is located on very hard soil (V_s>1000 m/sec), while thick and soft sediments covers downtown Adapazari.

The geotechnical data of the selected sites are shown in Table 2. Mean values of porosity and permeability are assumed equal to 0.4 and 10^{-7} m/s, respectively.

The earthquake generated a large number of ground-motion recordings within 200 km of the fault rupture. The E-W components of mainshock outcropping acceleration records at Sakarya station (Site E) is plotted in Fig. 7. The ground motion at downtown Adapazari during the mainshock was estimated to be two or three times larger than that of SKR. But it was hard to quantitatively interpret the variation of ground motion severity and its relation to earthquake damage due to the limitation on the surface geological and/or the geotechnical data near the strong motion observation sites and damaged areas (Kudo *et al.* 2000).

6.2 Estimation of ground motion in the Adapazari basin

In order to understand the damaging process and because no strong motion record was obtained in the fast-growing, it is intended in this section to estimate strong ground motion in this area incorporating the effects of porosity uncertainties. On other hand, in order to have a better insight of the contribution of soil conditions in

Table 3 Corrected (h, V_S, and ρ) and identified (ξ) characteristics values of the site of Adapazari (Khellafi *et al.* 2016)

Thickness (m)	Shear-wave velocity (m/s)	Mass density (kg/m^3)	Damping (%)
13.0	210	1670	0.3
23.5	260	1750	0.2
27.0	250	1740	0.9
28.0	540	1780	0.6
29.5	470	1760	0.3
33.0	530	1770	4.3
83.5	1070	2040	3.1
83.0	1040	2010	3.9
90.0	1050	2030	5.8
Bedrock	3500	2500	1.0

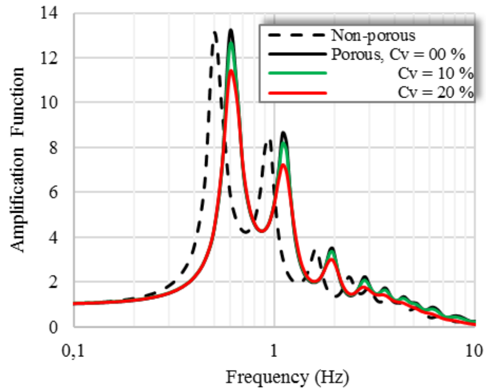

(a) for experimental data

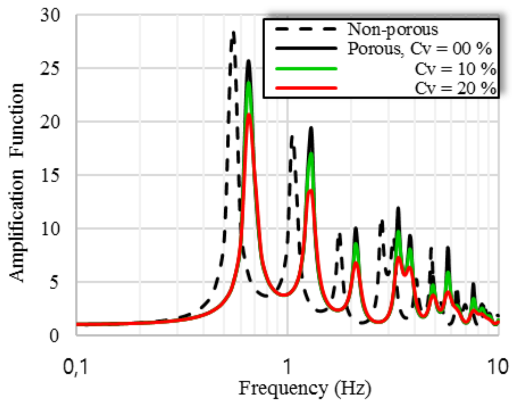

(b) for identified data

Fig. 8 Effects of porosity uncertainties on the mean amplification function of the Adapazarı multilayer site

estimated Adapazari's ground motions, corrected soil characteristics and identified damping ratios of all soil layers of the soil profile of Adapazari (site F) obtained by an inverse analysis (Khellafi *et al.* 2016) are used (Table 3). The amplification functions corresponding to the experimental data (Table 2) and to the identified data (Table 3) are plotted in Figs. 8(a) and 8(b), respectively, for random variations of porosity.

The increase of random variations of porosity (Fig. 8) decreases the amplitude of the amplification function as in the single layer soil profile case. For 20% C_v of porosity, the

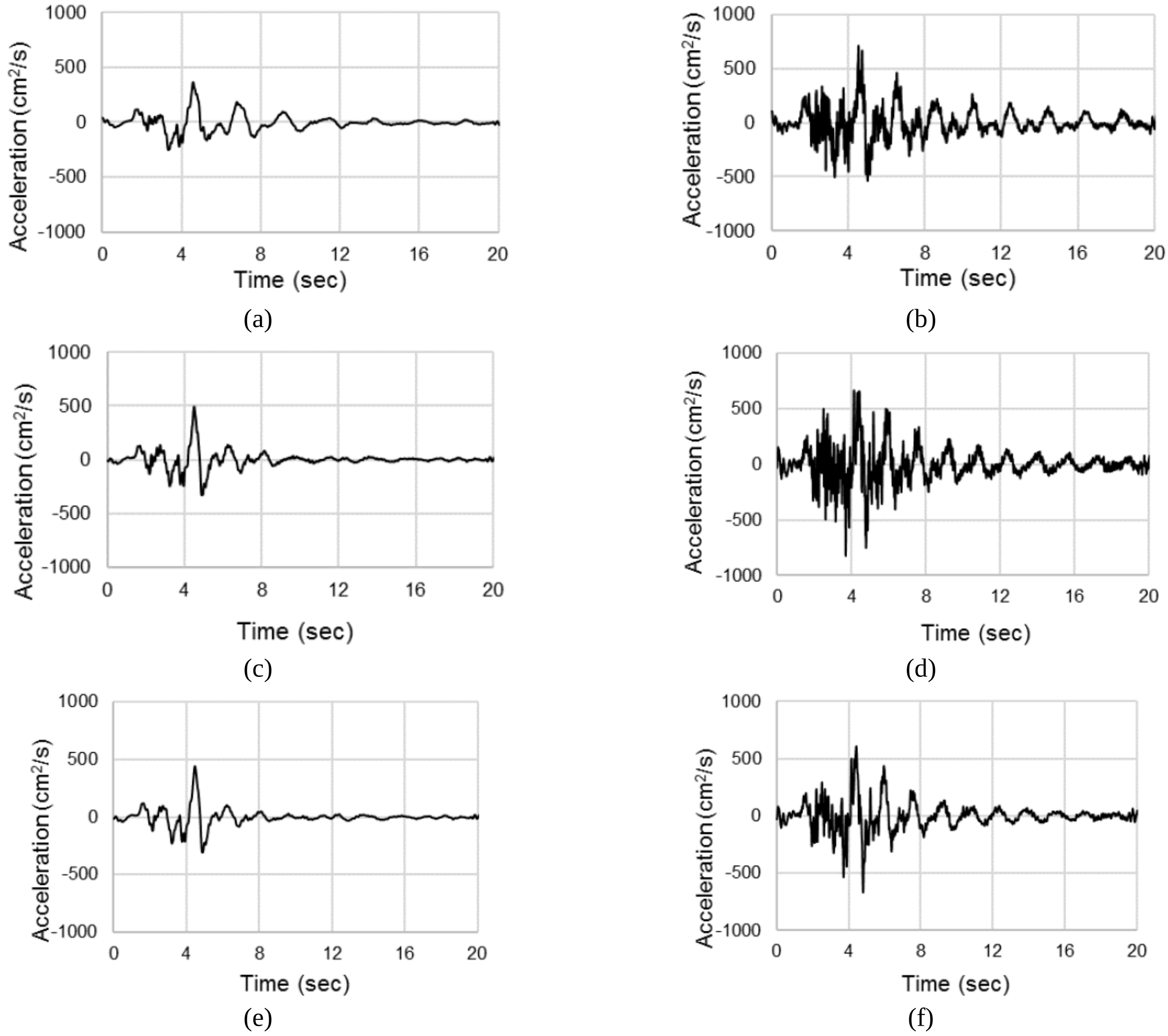

Fig. 9 Estimated ground surface accelerations at free surface of Adapazari site: (a) non-porous with experimental data, (b) no-porous with identified data, (c) Porous with experimental data and deterministic porosity, (d) Porous with identified data and deterministic porosity, (e) Porous with experimental data and random porosity, (f) Porous with identified data and random porosity

amplification function amplitude attenuates at the fundamental frequency (0.6 Hz) about 14% and 20% for the experimental and identified data, respectively.

Fig. 8(b) shows that the magnitudes of the amplification function obtained using identified data are significantly higher than that obtained with experimental data (Fig. 8(a)) due to low identified damping values but fundamental frequencies are preserved. This observation may explain the long duration of the shaking observed in SKR record motion (Erdik 2000) because of the multiple reflections and refractions at the layers' interfaces. After the amplification function is obtained, the EW component of the ground motion at SKR (Fig. 7) is deconvoluted at the Adapazari base rock in order to be used as an excitation input motion to estimate ground surface accelerations at Adapazari site.

The time acceleration histories at the free surface of the studied site corresponding to the non-porous case (Figs. 9(a)-(b)) and for the porous case (Figs. 9(c)-(d)) are obtained and compared for both experimental and identified parameters. From Fig. 9, it can be noted that when the soil profile of the Adapazari site is considered non-porous, its maximum ground surface accelerations are 0.37 g and 0.49 g for experimental and identified data, respectively. However, when porosity is included (ϕ=0.4), the peak ground surface accelerations at the same site increase up the 0.71 g and 0.82 g for experimental and identified data, respectively. The 0.82 g peak ground surface acceleration is close to that obtained by Khellafi *et al.* (2016) by an inverse analysis stochastic approach and agrees with the high building damage at the downtown of Adapazari. But when the porosity is considered as random variable with C_v value of 20% (Figs. 9(a)-(b)), the peak ground surface accelerations is reduced to 0.45 g and 0.66 g for experimental and identified data, respectively. The following conclusions may be addressed:

(i) under the assumption of non-porous media, the peak ground acceleration obtained with experimental data is moderate (0.37 g) but less than that obtained with identified data (0.49 g) nonetheless both do not agree with the high damage level observed in this area,

(ii) acceleration history for identified data present more peaks due to the multiples reflections and refraction of seismic waves at layers' interfaces and peak values are higher because of low identified damping values as shown by the multiple peaks in Fig. 8(b),

(iii) under the assumption of porous media, the peak ground accelerations reach very high values (Figs. 9(c)-(d)) and concord with the liquefaction-induced ground deformation observed in this area,

(iv) under the assumption of porous media with random porosity, the peak ground accelerations are reduced (Figs. 9(e)-(f)) compared to the non-porous case (Figs. 9(a)-(b)).

Therefore, site response analysis at Adapazari site in the framework of seismic wave propagation in porous media with uncertain porosity allowed a better insight of the damage process in this area due the 1999 Kocaeli earthquake shaking.

7. Conclusions

In this paper, it was intended to study the effect of soil properties' uncertainties on the response of anisotropic layered porous media with the help of Monte Carlo Simulations.

Firstly, the dispersion equation of *Love* wave was investigated. Then, soil amplifications due to the propagation of *SH*-body waves were studied and discussed. Lastly, this approach was applied to estimate ground motions at Adapazarı town city in Turkey lacked during the 1999 Kocaeli Earthquake mainshock.

The present study showed that soil properties uncertainties, namely porosity and permeability, considered in the framework of random fields described by probability distribution functions and statistical moments (mean value and coefficient of variation), significantly alter the wave propagation in porous media. Likewise, *Love* waves are more dispersive in porous media and the assumption of random porosity of the layer over the bedrock changes the zeros of the wave equation so that the velocity of the soil layer approaches that of the half-space for higher level of coefficient of variation (80%).

On other hand, random variations of porosity reduce the amplitudes of amplification functions, particularly nearby fundamental frequencies, while random variations of permeability do not exert significant effects on amplification functions.

Lastly, the application of the formulation of the seismic shear wave propagation in porous media to the Adapazari site in Turkey allowed the obtaining of the strong ground motion acceleration histories lacked during the main shock of the 1999 Kocaeli Earthquake. The obtained results are concordant with the high level of damage recorded in this area and the liquefaction-inducing ground deformation. However, more refined results need deeper investigations.

Other parameters such as the level of saturation and mechanical parameters of the solid skeleton on the behavior of a porous medium may illuminate about the appropriate model to investigate the response of porous media in such environment.

References

Assimaki, D., Pecker, A., Popescu, R. and Prevost, J. (2003), "Effects of spatial variability of soil properties on surface ground motion", *J. Earthq. Eng.*, **7**, 1-44.

Bansal, S.R. and Kuldeepak. (2011), "Study of propagation of shear waves in a multilayer medium including a fluid-saturated porous stratum", *Int. J. Theor. Appl. Sci*., **3**, 57-61.

Bezih, K., Chateauneuf, A., Kalla, M. and Bacconnet, C. (2015), "Effect of soil-structure interaction on the reliability of reinforced concrete bridges", *Ain Shams Eng. J.*, **1**, 2090-4479.

Biot, M.A. (1956a), "Theory of propagation of elastic waves in fluid-saturated porous solid. I. Low-frequency range", *J. Acoust. Soc. Am.*, **28**, 168-178.

Biot, M.A. (1956b), "Theory of propagation of elastic waves in a fluid-saturated porous solid. II. Higher frequency range", *J. Acoust. Soc. Am.*, **28**, 179-191.

Celebi, M., Toprak, S. and Holzer, T. (2000), "Strong-motion, site-effects and Hazard Issues in rebuilding Turkey: in light of the 17 August 1999 earthquake and its aftershocks", *Int. J. Hous. Sci. Its Appl.*, **24**, 21-38.

Cetin, K.O., Youd, T.L., Seed, R.B., Bray, J.D., Sancio, R., Lettis, W., ... & Durgunoglu, H.T. (2002), "Liquefaction-induced ground deformations at Hotel Sapanca during Kocaeli (Izmit), Turkey earthquake", *Soil Dyn. Earthq. Eng.*, **22**, 1083-92.

Crampin, S. (1970), "The dispersion of surface waves in multilayered anisotropic media", *Geophys. J. Int.*, **21**, 387-402.

Erdik, M. (2000), "Report on 1999 kocaeli and düzce (turkey) earthquakes", Bogazici University, Turkey.

Ghorai, A.P., Samal, S.K. and Mahanti, N.C. (2010), "Love waves in a fluid-saturated porous layer under a rigid boundary and lying over an elastic half-space under gravity", *Appl. Math. Model.*, **34**, 1873-1883.

Guellil, M.E., Harichane, Z., Berkane, H.D. and Sadouki, A. (2017), "Soil and structure uncertainly on the Foundation Structure dynamic response", *Earthq. Struct.*, **12**, 153-163.

Gupta, S., Vishwakarma, S.K., Majhi, D.K. and Kundu, S. (2013), "Possibility of Love wave propagation in a porous layer under the effect of linearly varying directional rigidities", *Appl. Math. Model.*, **37**, 6652-6660.

Kakar, R. (2015)," SH-wave propagation in a heterogeneous layer over an inhomogeneous isotropic elastic half-space", *Earthq. Struct.*, **9**(2), 305-320.

Khellafi, M.A., Harichane, Z., Afra, H. and Erken, A. (2016), "Prediction of parameters of soil stratums and earthen dams from free field acceleration records", *Int. J. Geotech. Earthq. Eng. (IJGEE)*, **7**, 33-56.

Kiełczyński, P. (2018), "Surface Love waves in a lossy layered planar waveguide with a viscoelastic guiding layer", *Appl. Math. Model.*, **53**, 419-432.

Kielczynski, P., Szalewski, M., Balcerzak, A. and Wieja, K. (2015), "Group and phase velocity of Love waves propagating in elastic functionally graded materials", *Arch. Acoust.*, **40**, 273-281.

Komazawa, M., Morikawa, H., Nakamura, K., Akamatsu, J., Nishimura, K., Sawada, S., Erken, A. and Onalp, A. (2002), "Bedrock structure in Adapazari, Turkey - a possible cause of severe damage by the 1999 Kocaeli earthquake", *Soil Dyn. Earthq. Eng.*, **22**, 829-836.

Kudo, K., Kanno, T., Okada, H., Özel, O., Erdik, M., Takahashi, M., Sasatani, T., Higashi, S. and Yoshida, K. (2000) "Site specific issues on strong ground motion during the Kociaeli, Turkey earthquake of August 17, 1999, as Inferred from Array Observations of Microtremors and Aftershocks", *Bull. Seismol. Soc. Am.*, **92**, 448-465.

Pallavika, V.K.K., Chakraborty, S.K. and Amalendu, S. (2008), "Finite difference modeling of SH-wave propagation in multilayered porous crust", *J. Ind. Geophys. Union.*, **12**, 165-172.

Rao Rama, Y.V. and Sarma, K.S. (1984), "Generation of SH type of waves due to stress discontinuity in a poroelastic-layered medium", *Ind. Inst. Sci.*, **64**, 21-28.

Ren, H., Goloshubin, G. and Hilterman, F.J. (2009), "Poroelastic analysis of amplitude-versus-frequency variations", *Geophys.*, **74**, 41-48.

Rohan, E. (2013), "Homogenization of acoustic waves in strongly heterogeneous porous structures", *Wave Motion*, **50**, 1073-1089.

Saha, A., Kundu, S., Gupta, S. and Vaishnav, P.K. (2015), "Love waves in a heterogeneous orthotropic layer under initial stress overlying a gravitating porous half-space", *Proc. Ind. Natn. Sci. Acad*., **81**, 1193-1205.

Sharma, M.D. and Gogna, M.L. (1993), "Reflection and transmission of SH waves in an initially stressed medium consisting of a sandy layer lying over a fluid-saturated porous solid", *Pageoph*, **140**, 613-628.

Sidhu, R.S. (1971), "Propagation of love waves in a two-layered heterogeneous half space", *Pageoph*., **91**(1), 76-94.

Son, M.S. and Kang, Y.J. (2012), "Propagation of shear waves in a poroelastic layer constrained between two elastic layers", *Appl. Math. Model.*, **36**, 3685-3695.

Wang, S. and Hao, H. (2002), "Effect of random variations of soil properties on site amplification of seismic ground motions", *Soil Dyn. Earthq. Eng.*, **22**, 551-64.

CC